Computing the mobility of grain boundaries

KOENRAAD G. F. JANSSENS[1,2]*****, **DAVID OLMSTED**[1], **ELIZABETH A. HOLM**[1], **STEPHEN M. FOILES**[1], **STEVEN J. PLIMPTON**[1] **AND PETER M. DERLET**[3]

[1]Sandia National Laboratories, PO Box 5800 MS 1411, Albuquerque, New Mexico 87185, USA
[2]Swiss Federal Institute of Technology, Institute for Virtual Manufacturing, Tannenstrasse 3, CH-8092 Zurich, Switzerland
[3]Paul Scherrer Institute, CH-5232 Villigen, Switzerland
*e-mail: janssens@ivp.mavt.ethz.ch

As current experimental and simulation methods cannot determine the mobility of flat boundaries across the large misorientation phase space, we have developed a computational method for imposing an artificial driving force on boundaries. In a molecular dynamics simulation, this allows us to go beyond the inherent timescale restrictions of the technique and induce non-negligible motion in flat boundaries of arbitrary misorientation. For different series of symmetric boundaries, we find both expected and unexpected results. In general, mobility increases as the grain boundary plane deviates from (111), but high-coincidence and low-angle boundaries represent special cases. These results agree with and enrich experimental observations.

Many modern technical materials are designed and manufactured by controlling the evolution of the microstructure using external influences such as heat or deformation. Independent of the class of material (nanomaterials, semiconductors, ceramics, metals and alloys, and some types of polymer), a microstructure, in essence, is a conglomerate of grains with varying crystallographic orientation. To control the evolution of the microstructure it is first brought to a state with an increased amount of stored energy (for example, by plastic deformation or irradiation). From that state the microstructure is annealed, carefully steering it to a configuration with the desired technical properties. Most of the solid-state microstructure transformations, such as recrystallization, grain growth, phase transformation or precipitation, involve the motion of grain boundaries. Grain boundary motion is a product of the driving pressure, which is a consequence of the energy stored in the microstructure, and the mobility of the grain boundary. Here we demonstrate how a molecular dynamics computation with a grain boundary potential energy formulation can be used to directly measure grain boundary mobility, which until now has proven to be time-consuming and difficult to compute or measure.

The mobility of a solid-state grain or phase boundary is determined by the atomistic mechanisms by which the boundary moves. Although uncertainty remains about the exact nature of these mechanisms, it is generally accepted that mobility strongly depends on the crystallographic misorientation between neighbouring grains.

Misorientation depends on five independent variables, three to represent the orientation difference between the crystal lattices and two for the grain boundary plane, which represents a substantial parameter space. It should be noted that the three translational degrees of freedom at the boundary are automatically minimized by the simulation method, just as they are in reality. In addition, it has proved challenging, if not impossible, to come up with a natural driving pressure to move and measure the grain boundary motion whilst keeping the grain boundary flat and its misorientation constant. Approaches that study flat boundaries (driven by volumetric driving forces such as stress or magnetism)[1–3] rely on special crystallographic anisotropies and thus have been fundamentally limited in the misorientations that can be studied.
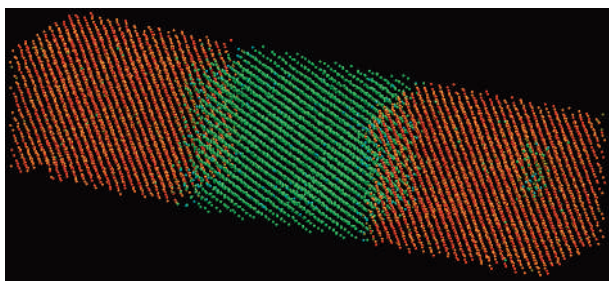
Figure 1 Example of a computational experiment for the mobility of a symmetric 55° [111] mixed-type grain boundary in f.c.c. aluminium. The atoms are coloured from red ($\xi_i = 0$) over green to blue ($\xi_i = \xi_i^{max}$). The simulated configuration is periodic for *x*, *y* and *z* directions. Note the vacancy (with a cloud of displaced green atoms surrounding it) in the upper right corner.

Methods that study curved boundaries[4–7] cannot single out a specific misorientation. State-of-the-art mesoscale computational methods[8–14] aimed at the prediction of the grain-scale evolution of polycrystalline microstructures are rapidly maturing to a state where they can be applied to materials of technical interest. Grain boundary mobility is an essential input parameter for these approaches, as without this parameter predictions are restricted to general scientific interest, but not applicable to the design of specific, technical microstructures. Using molecular dynamics to model the grain growth process itself[15,16] is limited in system size to a few nanoscale grains.

In this article we use an artificial, crystal-orientation-dependent driving pressure, introduced into an embedded atom molecular dynamics simulation, to compute the grain boundary mobility in a pure material: face-centred-cubic (f.c.c.) aluminium. This method permits calculation of grain boundary mobility for flat boundaries over the full range of crystallographic misorientation space. Preliminary results provide insights into grain boundary motion, some of which are surprising.

A crystal lattice with a specific orientation *I* implies that, ideally, each atom *i* with position vector $\mathbf{r}_i$ has its nearest-neighbour atoms *j* at specific positions $\mathbf{r}_j^I$. Any local deviation from that orientation results in nearest-neighbour positions $\mathbf{r}_j$. We define the order parameter ξ_i for each atom *i* as

$$\xi_i = \sum_j |\mathbf{r}_j - \mathbf{r}_j^I|,$$

where the sum is over the *N* nearest-neighbour atoms *j* of *i*, and $\mathbf{r}_j^I$ is the nearest ideal lattice site of crystal *I* to $\mathbf{r}_j$. *N* is 12 for the f.c.c. materials of this article. Note that ξ_i is zero if the local orientation is exactly *I*, and is positive for any deviation from that orientation.

Now consider an atom *i* in a perfect lattice with orientation *J*. The orientation difference between *I* and *J* can be expressed as an 'ideal' value (in the absence of defects and thermal vibrations)

$$\xi_{IJ} = \sum_j |\mathbf{r}_j^J - \mathbf{r}_j^I|$$

where $\mathbf{r}_j^J$ are the lattice sites in crystal *J* that neighbour atom *i*.

In a bicrystal system with grain A having orientation *I* and grain B having orientation *J*, we now add an orientation-dependent potential energy to the atoms that creates a driving pressure acting on the grain boundary. Such an artificial potential $u_\xi(\mathbf{r}_i)$ can be

defined at each atom *i* as

$$u_\xi(\mathbf{r}_i) = \begin{cases} 0 & \xi_i < \xi_l \\ \dfrac{V}{2}(1 - \cos 2\omega_i) & \text{with } \omega_i = \dfrac{\pi}{2}\dfrac{\xi_i - \xi_l}{\xi_h - \xi_l} \quad \xi_l < \xi_i < \xi_h \quad (1) \\ V & \xi_h < \xi_i \end{cases}$$

with $\xi_l = f\xi_{IJ}$ and $\xi_h = (1-f)\xi_{IJ}$. The $\cos\omega_i$ function is chosen such that its derivative is zero at ξ_l and ξ_h and shows a smooth transition between those two values. The value of the fraction *f* is chosen to reduce the effect of the artificial potential on the normal thermal vibrations of the atoms around their lattice sites, and ensures that the added energy is free energy. The optimal value of *f* depends on the material, potential and temperature. The effect of $u_\xi(\mathbf{r}_i)$ is that atoms of grain B far from the AB interface now have a potential energy larger than the potential energy of grain A atoms by a value of *V* per atom. This potential energy difference goes to zero as an atom's coordinates cross the bicrystal interface from B to A. This is the equivalent of grain B containing a stored energy; consequently, atoms near the interface will be driven into a grain A orientation and the grain boundary will migrate into grain B. The extra force on each atom is given by

$$\mathbf{F}(\mathbf{r}_i) = -\frac{\partial u_\xi}{\partial \mathbf{r}_i} = -\frac{\pi V}{2(\xi_h - \xi_l)}\left\{\left(\sum_j \frac{\boldsymbol{\delta}_{ij}}{|\boldsymbol{\delta}_{ij}|}\right)\sin 2\omega_i \right.$$
$$\left. + \sum_j\left[-\frac{\boldsymbol{\delta}_{ji}}{|\boldsymbol{\delta}_{ji}|}\sin 2\omega_j\right]\right\} \quad \text{for } \xi_l < \xi_i, \xi_j < \xi_h,$$

where $\boldsymbol{\delta}_{ij} = \mathbf{r}_i + \mathbf{I}_{ij} - \mathbf{r}_j$ and $\mathbf{I}_{ij} = \mathbf{r}_j^I - \mathbf{r}_i$. For ξ_i and ξ_j outside the given limits $\mathbf{F}(\mathbf{r}_i)$ is a zero length vector. In these simulations, we use as our baseline potential an embedded atom method (EAM) potential for aluminium published in ref. 17. We add equation (1) to that potential with $f = 0.25$ and *V* set as discussed below. This model has been implemented as an option in the LAMMPS molecular dynamics package[18,19]. Despite the 'artificial' nature of the extra driving force, this method is a conventional molecular dynamics implementation, which follows the relevant statistical mechanics rules. All atomic motion mechanisms, including thermal vibrations as well as random and directed motion along and across boundaries, are included, and detailed balance is maintained. In fact, our flat boundaries move analogously to any flat boundary experiencing a volumetric driving force; the only difference is that our driving force does not arise from a physical cause such as stress or a magnetic field but rather is applied synthetically.

Figure 1 shows an example of a computational experiment on a fully periodic system of about 26,000 atoms (a range between 14,000 and 150,000 was used for the runs discussed here). Note that, owing to the simpler geometry of the current simulations, this system size is considerably smaller than required for curvature-driven molecular dynamics simulations[5]. The grain at the ends is set to orientation *I*, the grain in the middle to orientation *J* and the artificial potential energy term is added to all atoms. As a consequence both grain boundaries move towards the centre of the sample during a molecular dynamics run of 100 ps in timesteps of 0.001 ps, as illustrated by the plot of Fig. 2. (If *I* and *J* were reversed, both grain boundaries would move away from the centre.) Figure 2 shows that boundary velocity is constant throughout the simulation, as expected in a constant driving pressure system, and is about the same for both boundaries. We can calculate the boundary mobility by dividing this constant velocity by the driving pressure assuming the nominal lattice constant of 4.032 Å.

To study mobility as a function of misorientation angle, we examined several boundary series at a temperature of 800 K.
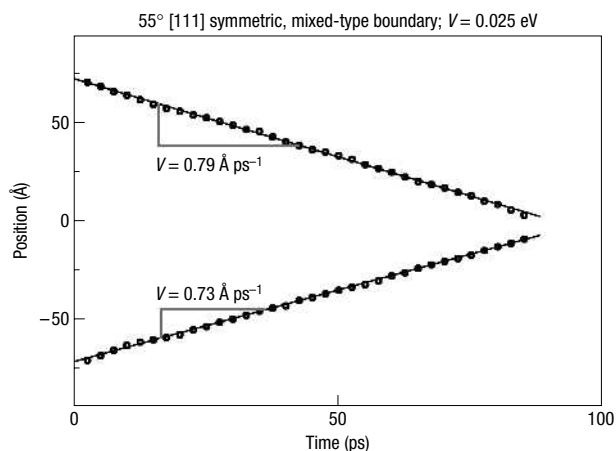
Figure 2 Example of the grain boundary motion at 800 K and $V = 0.025$ eV for the sample shown in Fig. 1.

Figure 3 Mobility of aluminium grain boundaries at 800 K with different misorientation angles around a [111]-type axis and various grain boundary planes. For some misorientations the normal to the grain boundary plane is indicated. The boundaries are all symmetric, meaning that the boundary plane type is the same with respect to both crystals, for example, [61$\bar{1}$] and [16$\bar{1}$] for the 30° misorientation angle. The angle between the misorientation axis and the boundary normal is 54.74° for all mixed boundaries shown. The values shown are an average derived from the velocities of the left and right grain boundaries, both moving towards the sample centre.

Series A includes symmetric [111] pure twist boundaries; that is, the boundary plane is exactly (111) and the misorientation angle represents a rotation about [111]. Here, $V = 0.025$ eV per atom (equivalent to 244 MPa, which is about 25 times the maximum driving pressure in highly deformed metals). Figure 3 shows near-zero mobility for the exact $\Sigma 3$ twin boundary (60° about [111]) and somewhat low mobility for the exact $\Sigma 7$ coincident site lattice (CSL) boundary (38.21° about [111]), both in agreement with experiment[20]. Although the mobility minimum near the $\Sigma 3$ boundary is quite flat (even 55° misorientation boundaries have near-zero mobility), the $\Sigma 7$ boundary is a mobility cusp, with near-$\Sigma 7$ boundaries higher in mobility than the exact CSL misorientation. This agrees with experimental observations that show near-$\Sigma 7$ boundaries move quickly whereas near-$\Sigma 3$ boundaries are immobile[21].

Series B and C are data from 100-ps molecular dynamics runs of symmetric, mixed-type boundaries; that is, the [111] misorientation axis is neither parallel nor perpendicular to the grain boundary plane, and the grain boundary plane deviates from (111). These results surprisingly show that some grain boundaries with a $\Sigma 3$-type misorientation axis–angle pair have very high mobility relative to other boundaries. In other simulations, we have observed $\Sigma 3$ mixed-type boundaries that are of intermediate mobility. Taken together, these results indicate that although some $\Sigma 3$ boundaries, including the symmetric twin, are essentially immobile, other $\Sigma 3$ boundaries may be exceptionally mobile. In fact, the mobility of nominal $\Sigma 3$ boundaries varies by orders of magnitude as the boundary plane changes. Although nearly all research published on this subject, experimental or computational, neglects the dependence of the mobility on the boundary plane normal, our results indicate that this assumption is incorrect. In fact, two boundaries with precisely the same misorientation angle–axis pair but different boundary planes have the smallest and the largest mobilities observed in our simulations. Not only is this result interesting in itself, it could also affect grain boundary engineering processes that strive to maximize $\Sigma 3$ boundary content in metallic microstructures[22].

The near-$\Sigma 7$ 40° [111] boundary has been reported to possess an anomalously high mobility[23], and this observation is often used in theories for abnormal grain growth. Our results for both pure twist and mixed boundaries do not show a particularly high mobility for such boundaries. In fact, the exact $\Sigma 7$ twist boundary has a rather low mobility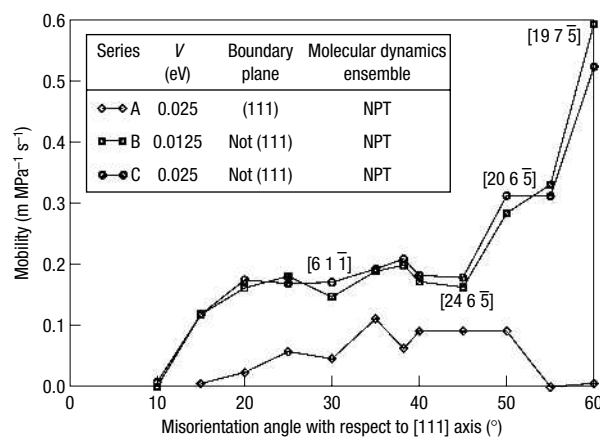, and although the mobility of the mixed-type $\Sigma 7$ boundary is higher, it is similar to that of other high-angle boundaries. The experimental results concern the boundary mobility of a new grain growing into a deformed microstructure, and as the authors note, the mobility peak at 40° [111] occurs only when the grain boundary plane normal is perpendicular to the active deformational cross slip system[23]. As such, we must conclude that the higher growth rate observed for near-$\Sigma 7$ 40° [111] boundaries is specific to the deformation structure, and not specific to the misorientation of the boundary. Furthermore, in comparing with experiments, the effect of solutes, even in very small amounts, cannot be discounted.

Series B and C also illustrate that the mobility is independent of the magnitude of the driving pressure, at least within the ranges tested. We also observed that the mobility did not vary with the thermodynamic ensemble studied; NPT simulations (in which the number of molecules, pressure and temperature are constant, shown here) gave nearly identical results to NVE simulations (in which the number of molecules, the system volume and the total energy are constant). The mobility of mixed-type boundaries is notably higher than the mobility for the pure twist type boundaries, which is not unexpected, as these boundaries are more disordered[24,25]. These results agree with observations and assumptions that, in general, mobility increases as the grain boundary plane is angularly further from a [111]-type plane.

The simulations also confirm that for low-angle grain boundaries, the mobility rapidly drops. The transition between low-angle and high-angle boundary behaviour is typically assumed to occur around 13°, which agrees with our data for mixed-type boundaries. However, for pure twist boundaries this transition seems to occur much more gradually, and low mobility persists beyond 20°. Finally, we note that these results are within an order of magnitude of those observed in experiments, where the grain boundary mobility in high-purity aluminium at 800 K is typically about 0.04 m MPa^{-1} s^{-1} (ref. 26); our mobilities are somewhat larger than experimental values, consistent with other molecular dynamics studies[1,5].

Quantitative measurement of grain boundary mobilities is critical to modelling the annealing process in materials ranging from nanomaterials to crystalline polymers. However, current experimental and simulation methods cannot determine mobility for flat boundaries across the large misorientation phase space. We have developed an orientation-dependent atomistic potential that produces an artificial driving force on atoms near boundaries. When used in molecular dynamics simulations, this allows us to induce motion in flat boundaries of arbitrary misorientation using considerably smaller systems and shorter simulation timescales than previously attainable. For a given boundary, we find that boundary velocity is constant over a range of simulation parameters: this permits us to calculate the boundary mobility. For different series of symmetric boundaries, we find both expected results (high-coincidence (111) twist boundaries such as the Σ3 twin are of very low mobility) and unexpected results (some mixed boundaries of the Σ3 misorientation are of very high mobility). In general, mobility increases as the grain boundary plane deviates from (111). Furthermore, we observe that although some boundaries represent a cusp in mobility space (for example, Σ7 pure twist boundaries), others occupy gradual wells in the mobility profile (for example, low-angle boundaries, Σ3 twin boundaries). Although these results are in general agreement with experimental observations, they add detail that has not been observed before.

Grain boundary parameter space is vast and these results merely scratch the surface. Further simulations will examine ⟨111⟩ tilt boundaries, the temperature dependence of boundary mobility and mobility in different material systems. However, even these preliminary results provide insight into, and further questions about, grain boundary mobility in f.c.c. metals.

References

1. Zhang, H., Mendelev, M. I. & Srolovitz, D. J. Computer simulation of the elastically driven migration of a flat grain boundary. *Acta Mater.* **52,** 2569–2576 (2004).
2. Huang, Y. & Humphreys, F. J. Measurements of grain boundary mobility during recrystallization of a single-phase aluminium alloy. *Acta Mater.* **47,** 2259–2268 (1999).
3. Winning, M., Gottstein, G. & Shvindlerman, L. S. On the mechanisms of grain boundary migration. *Acta Mater.* **50,** 353–363 (2002).
4. Upmanyu, M., Srolovitz, D. J., Shvindlerman, L. S. & Gottstein, G. Molecular dynamics simulation of triple junction migration. *Acta Mater.* **50,** 1405–1420 (2002).
5. Zhang, H., Upmanyu, M. & Srolovitz, D. J. Curvature driven grain boundary migration in aluminum: molecular dynamics simulations. *Acta Mater.* **53,** 79–86 (2005).
6. Adams, B. L., Kinderlehrer, D., Mullins, W. W., Rollett, A. D. & Ta'asan, S. Extracting the relative grain boundary free energy and mobility functions from the geometry of microstructures. *Scripta Mater.* **38,** 531–536 (1998).
7. Saylor, D. M., Morawiec, A. & Rohrer, G. S. The relative free energies of grain boundaries in magnesia as a function of five macroscopic parameters. *Acta Mater.* **51,** 3675–3868 (2003).
8. Janssens, K. G. F. Three dimensional space-time coupled cellular automata for the simulation of recrystallization and grain growth. *Model. Simul. Mater. Sci.* **11,** 157–171 (2003).
9. Anderson, P., Grest, G. S. & Srolovitz, D. J. Computer simulation of normal grain growth in three dimensions. *Phil. Mag. B* **59,** 293–329 (1989).
10. Rollett, A. D. & Raabe, D. A hybrid model for mesoscopic simulation of recrystallization. *Comp. Mater. Sci.* **21,** 69–78 (2001).
11. Krill, C. E. III & Chen, L. Q. Computer simulation of 3-D grain growth using a phase-field model. *Acta Mater.* **50,** 3057–3073 (2002).
12. Kuprat, A., George, D., Straub, G. & Demirel, M. C. Modeling microstructure evolution in three dimensions with Grain3D and LaGriT. *Comp. Mater. Sci.* **28,** 199–208 (2003).
13. Raabe, D., Roters, F., Barlat, F. & Chen, L.-Q. *Continuum Scale Simulation of Engineering Materials: Fundamentals - Microstructures - Process Applications* (Wiley-VCH, Weinheim, 2004).
14. Sethian, J. A. *Level Set Methods and Fast Marching Methods* (Cambridge Univ. Press, Cambridge, 2002).
15. Van Swygenhoven, H., Farkas, D. & Caro, A. Grain boundary structures in polycrystalline metals at the nanoscale. *Phys. Rev. B* **62,** 831–838 (2000).
16. Schonfelder, B., Wolf, D., Phillpot, S. R. & Furtkamp, M. Molecular-dynamics method for the simulation of grain-boundary migration. *Interface Sci.* **5,** 245–262 (1997).
17. Ercolessi, F. & Adams, J. B. Interatomic potentials from 1st principles calculations—the force matching method. *Europhys. Lett.* **26,** 583–588 (1994).
18. Plimpton, S. J. Fast parallel algorithms for short-range molecular dynamics. *J. Comp. Phys.* **117,** 1–19 (1995).
19. http://www.cs.sandia.gov/~sjplimp/lammps.html.
20. Gottstein, G. & Shvindlerman, L. S. *Grain Boundary Migration in Metals: Thermodynamics, Kinetics, Applications* (CRC, Boca Raton, Florida, 1999).
21. Humphreys, F. J. & Hatherly, M. *Recrystallization and Related Annealing Phenomena* (Pergamon, Oxford, 1996).
22. Palumbo, G., Lehockey, E. M. & Lin, P. Applications for grain boundary engineered materials. *JOM* **50,** 40–43 (1998).
23. Liebmann, B., Lücke, K., Graham, C. D., Cahn, R. W. & Dunn, C. G. Grain growth rates and orientation relationships in the recrystallization of aluminum single crystals. *Trans. AIME* **206,** 1413–1416 (1956).
24. Gleiter, H. The mechanism of grain boundary migration. *Acta Metall.* **17,** 565–573 (1969).
25. Gleiter, H. Theory of grain boundary migration rate. *Acta Metall.* **17,** 853–862 (1969).
26. Shvindlerman, L. S., Gottstein, G. & Molodov, D. A. Grain boundary motion in pure metals: effect of interaction between adsorbed atoms at moving boundaries. *Phys. Status Solidi A* **160,** 419–429 (1997).

Competing financial interests

The authors declare that they have no competing financial interests.